

Significant Improvement of Semiconducting Performance of the Diketopyrrolopyrrole-Quaterthiophene Conjugated Polymer through Side-Chain Engineering via Hydrogen-Bonding

Jingjing Yao, Chenmin Yu, Zitong Liu,* Hwei Luo, Yang Yang, Guanxin Zhang, Deqing
Zhang*

Beijing National Laboratory for Molecular Sciences, Organic Solids Laboratory, Institute
of Chemistry, Chinese Academy of Sciences, Beijing 100190, China

E-mail: dqzhang@iccas.ac.cn

1. Thermogravimetric Analysis (TGA) and Differential Scanning Calorimetry (DSC) Curves	S2
2. Cyclic Voltammograms	S2
3. Synthesis and Characterization of pDPP4T , pDPP4T-A , pDPP4T-B and pDPP4T-C . S3	
4. HOMO/LUMO Energies and Band Gaps of pDPP4T-A , pDPP4T-B and pDPP4T-C . S5	
5. Fabrication of FET Devices	S6
6. Transfer and Output Curves of BGBC and BGTC Devices with Thin Films of pDPP4T-1 , pDPP4T-2 , pDPP4T-3 , pDPP4T , pDPP4T-A , pDPP4T-B and pDPP4T-C	S8
7. Devices Stability Data.....	S10
8. 1-D GIXRD Patterns.....	S10
9. AFM Images of pDPP4T-A , pDPP4T-B and pDPP4T-C	S12
10. Fabrication of Organic Photovoltaic Cells.....	S12
11. <i>J-V</i> Curves and IPCE Spectra of pDPP4T-A , pDPP4T-B and pDPP4T-C with PC ₇₁ BM	S13
12. ¹ HNMR and ¹³ CNMR Spectra	S14

1. Thermogravimetric Analysis (TGA) and Differential Scanning Calorimetry (DSC) Curves

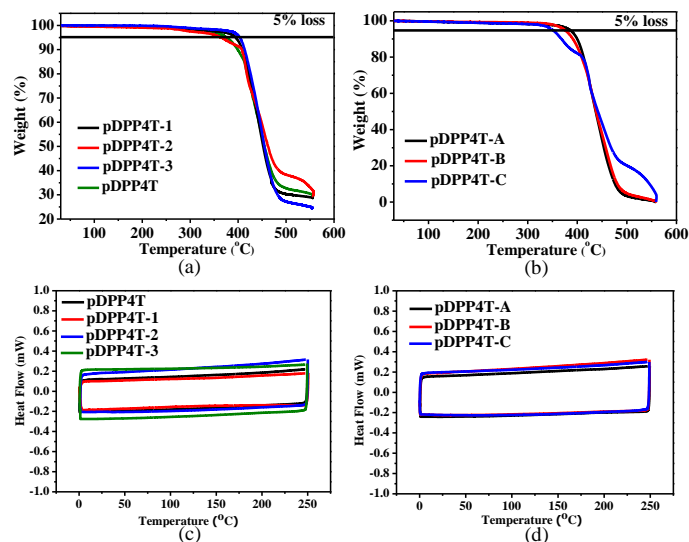


Figure S1. (a-b) TGA curves of **pDPP4T-1**, **pDPP4T-2**, **pDPP4T-3**, **pDPP4T**, **pDPP4T-A**, **pDPP4T-B** and **pDPP4T-C**: heating rate: 10 °C/min. From 25 °C to 550 °C under nitrogen atmosphere; (c-d) DSC curves (endo up) of **pDPP4T-1**, **pDPP4T-2**, **pDPP4T-3**, **pDPP4T**, **pDPP4T-A**, **pDPP4T-B** and **pDPP4T-C** recorded at a heating and cooling rate (0-250 °C) of 10 °C/min under nitrogen.

2. Cyclic Voltammograms

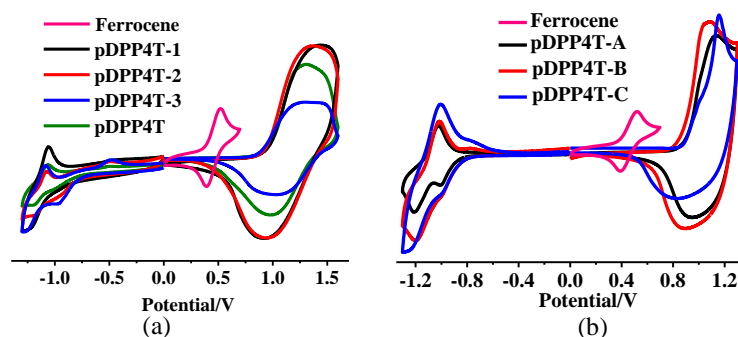
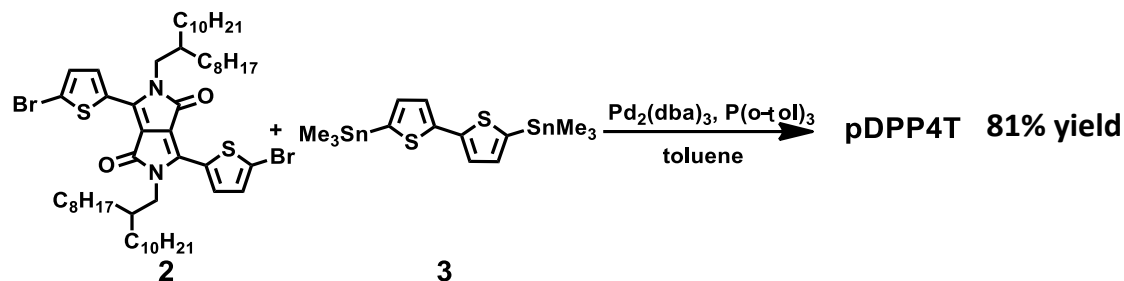
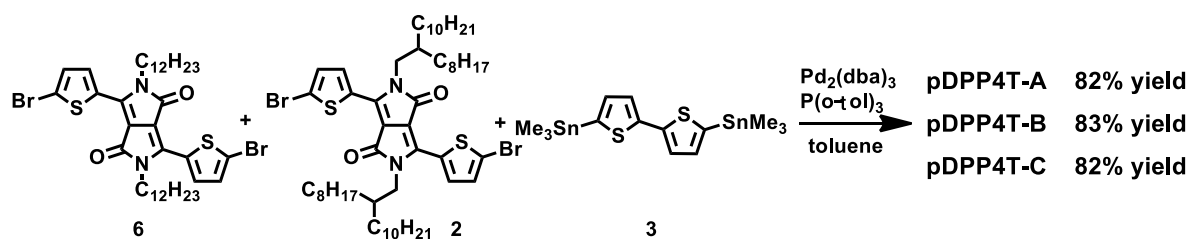


Figure S2. Cyclic voltammograms of **pDPP4T-1**, **pDPP4T-2**, **pDPP4T-3**, **pDPP4T**, **pDPP4T-A**, **pDPP4T-B** and **pDPP4T-C** films at a scan rate of 100 mVs⁻¹. Pt was used as working electrode and counter electrode and Ag/AgCl (saturated KCl) as reference electrode; *n*-Bu₄NPF₆ (0.1 M) in CH₃CN as supporting electrolyte. For calibration, the redox potential of ferrocene/ferrocenium (Fc/Fc⁺) was measured under the same conditions.

3. Synthesis and Characterization of pDPP4T, pDPP4T-A, pDPP4T-B and pDPP4T-C



Synthesis of pDPP4T. Compound **2** (101.9 mg, 0.10 mmol), compound **3** (49.2 mg, 0.10 mmol), $\text{P}(o\text{-tol})_3$ (4.9 mg, 0.016 mmol) and $\text{Pd}_2(\text{dba})_3$ (1.8 mg, 0.0020 mmol) were used. The purified polymer was collected to give deep green solid (83.3 mg, 81% yield). ^1H NMR (500 MHz, 1,1,2,2-tetrachloroethane- d_2 , 100 °C): δ 8.98-8.92 (m, br, 2H), 7.31-6.94 (m, br, 6H), 4.09-4.02 (m, br, 4H), 2.18-2.03 (m, br, 10H), 1.30 (s, 56H), 0.92 (s, 12H); ^{13}C NMR (100 MHz, solid): δ 160.09, 140.33, 136.05, 128.04, 123.69, 107.94, 45.24, 38.36, 32.08, 30.09, 23.05, 14.41; M_w/M_n (GPC) = 40.2/18.8 kg mol $^{-1}$. Anal. calcd for $(\text{C}_{62}\text{H}_{90}\text{N}_2\text{O}_2\text{S}_4)_n$: C, 72.75; H, 8.86; N, 2.74; S, 12.53. Found: C, 72.50; H, 8.92; N, 2.78; S, 12.39.



Synthesis of pDPP4T-A. Compound **6** (2.6 mg, 0.0033 mmol), compound **2** (101.9 mg, 0.10 mmol), compound **3** (50.7 mg, 0.10 mmol), $\text{P}(o\text{-tol})_3$ (5.0 mg, 0.016 mmol) and $\text{Pd}_2(\text{dba})_3$ (1.9 mg, 0.0021 mmol) were used. The purified polymer was collected to give deep green solid (86.7 mg, 82% yield). ^1H NMR (500 MHz, 1,1,2,2-tetrachloroethane- d_2 , 100 °C): δ 8.85 (s, br, 2H), 7.07-6.91 (m, br, 6H), 4.09 (s, br, 4H), 2.25-2.08 (m, br, 10H),

1.67-1.32 (m, br, 56H), 0.93 (s, 12H); ^{13}C NMR (100 MHz, solid): δ 160.91, 140.94, 137.32, 129.00, 124.76, 108.64, 45.08, 38.79, 37.63, 32.66, 30.58, 23.56, 14.88. M_w/M_n (GPC) = 211.6/74.0 kg mol $^{-1}$. Anal. calcd. for $(\text{C}_{1936}\text{H}_{2878}\text{N}_{62}\text{O}_{62}\text{S}_{124})_n$: C, 72.69; H, 9.07; N, 2.71; S, 12.43. Found: C, 72.27; H, 8.57; N, 2.82; S, 12.51.

Synthesis of pDPP4T-B. Compound **6** (4.0 mg, 0.0050 mmol), compound **2** (101.9 mg, 0.10 mmol), compound **3** (51.8 mg, 0.11 mmol), P(*o*-tol) $_3$ (5.1 mg, 0.017 mmol) and Pd $_2$ (dba) $_3$ (1.9 mg, 0.0021 mmol) were used. The purified polymer was collected to give deep green solid (88.7 mg, 83% yield). ^1H NMR (500 MHz, 1,1,2,2-tetrachloroethane- d_2 , 100 $^\circ\text{C}$): δ 8.89 (s, br, 2H), 7.08-6.93 (m, br, 6H), 4.09 (s, br, 4H), 2.25-2.07 (m, br, 10H), 1.69-1.32 (m, br, 56H), 0.93 (s, 12H); ^{13}C NMR (100 MHz, solid): δ 160.87, 141.25, 136.74, 128.59, 124.29, 108.37, 45.46, 38.73, 32.67, 30.72, 23.62, 14.94. M_w/M_n (GPC) = 190.9/91.5 kg mol $^{-1}$. Anal. calcd. for $(\text{C}_{1306}\text{H}_{1938}\text{N}_{42}\text{O}_{42}\text{S}_{84})_n$: C, 72.64; H, 9.05; N, 2.72; S, 12.47. Found: C, 71.89; H, 8.68; N, 2.80; S, 12.49.

Synthesis of pDPP4T-C. Compound **6** (8.0 mg, 0.010 mmol), compound **2** (101.9 mg, 0.10 mmol), compound **3** (54.1 mg, 0.11 mmol), P(*o*-tol) $_3$ (5.4 mg, 0.018mmol) and Pd $_2$ (dba) $_3$ (2.0 mg, 0.0022 mmol) were used. The purified polymer was collected to give deep green solid (92.2 mg, 82% yield). ^1H NMR (500 MHz, 1,1,2,2-tetrachloroethane- d_2 , 100 $^\circ\text{C}$): δ 8.99-8.90 (m, br, 2H), 7.14-6.97 (m, br, 6H), 4.11-4.00 (s, br, 4H), 2.10-2.06 (m, br, 10H), 1.47-1.33 (m, br, 56H), 0.92 (s, 12H); ^{13}C NMR (100 MHz, solid): δ 160.21, 140.49, 136.35, 128.20, 123.69, 108.09, 45.09, 38.55, 31.93, 30.14, 23.05, 14.39. M_w/M_n

(GPC) = 207.8/94.6 kg mol⁻¹. Anal. calcd. for (C₆₆₆H₉₅₈N₂₂O₂₂S₄₄)_n: C, 72.48; H, 8.75; N, 2.79; S, 12.78. Found: C, 72.46; H, 8.75; N, 2.50; S, 12.88.

4. HOMO/LUMO Energies and Band Gaps of pDPP4T-A, pDPP4T-B and pDPP4T-C

Table S1. Absorption, Onset Redox Potentials, HOMO/LUMO Energies and Band Gaps of pDPP4T-A, pDPP4T-B and pDPP4T-C.

polymer	λ_{\max}^a (nm)		$E_{\text{redl}}^{\text{onset}}$ (V) ^c	E_{LUMO} (eV) ^d	$E_{\text{oxl}}^{\text{onset}}$ (V) ^c	E_{HOMO} (eV) ^d	E_g^{cv} (eV) ^e	E_g^{opt} (eV) ^f
	($\epsilon_{\max}, \text{M}^{-1} \text{cm}^{-1}$) ^b							
	solution	film						
pDPP4T-A	784(80000)	726,784	-1.28	-3.52	0.47	-5.27	1.75	1.33
pDPP4T-B	788(82000)	726,790	-1.26	-3.54	0.46	-5.26	1.71	1.32
pDPP4T-C	800(83000)	726,790	-1.26	-3.54	0.46	-5.26	1.72	1.32

^a Absorption maxima in CHCl₃ solution (1.0×10⁻⁵ M for each polymer) and the spin-coated thin film; ^b Molar extinction coefficient ($\epsilon_{\max}, \text{M}^{-1} \text{cm}^{-1}$); ^c Onset potentials (V vs Fc/Fc⁺) for reduction ($E_{\text{redl}}^{\text{onset}}$) and oxidation ($E_{\text{oxl}}^{\text{onset}}$); ^d Estimated with the following equation: $E_{\text{HOMO}} = - (E_{\text{oxl}}^{\text{onset}} + 4.8) \text{ eV}$, $E_{\text{LUMO}} = - (E_{\text{redl}}^{\text{onset}} + 4.8) \text{ eV}$; ^e Based on redox potentials; ^f Based on the absorption spectral data.

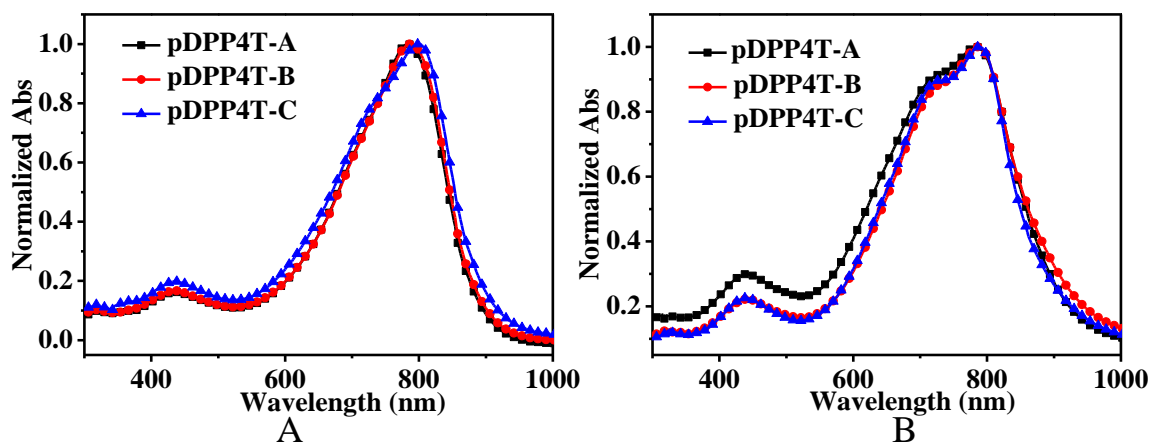


Figure S3. Normalized UV-vis absorption spectra of **pDPP4T-A**, **pDPP4T-B** and **pDPP4T-C** in CHCl₃ (1.0×10⁻⁵ M) (A) and their thin films (B).

5. Fabrication of FET Devices

Solutions of conjugated polymers were prepared by dissolving the copolymers in chloroform at a concentration of 7.0 mg/mL except **pDPP4T-C** (3.0 mg/mL in 1,1,2,2-tetrachloroethane). The typical polymer film thickness (around 40-45 nm) was measured on profilometer (Ambios Tech. XP-2). Bottom-Gate/Bottom-Contact FETs were fabricated. A heavily doped *n*-type Si wafer and a layer of dry oxidized SiO₂ (300 nm, with roughness lower than 0.1 nm and capacitance of 11 nF cm⁻²) were used as a gate electrode and gate dielectric layer, respectively. The drain-source (*D-S*) gold contacts (28 nm) were fabricated by photo-lithography. The substrates were first cleaned by sonication in acetone and water for 5.0 min and immersed in Piranha solution (2:1 mixture of sulfuric acid and 30% hydrogen peroxide) for 20 min. This was followed by rinsing with deionized water and isopropyl alcohol for several times, and it was blow-dried with nitrogen. Then, the surface was modified with *n*-octadecyltrichlorosilane (OTS). After that, the substrates were cleaned in *n*-hexane, CHCl₃ and isopropyl alcohol. The films of conjugated polymers were fabricated by spin-coating their solutions at 3000 rpm. The annealing process was carried out in vacuum for 1.0 h at each temperature.

The bottom-gate/top-contact devices with fabricated similarly except Au source/drain electrodes (50 nm) were deposited via thermal vacuum evaporation through a shadow mask after spin coating the semiconductor solution and then annealed at different temperatures in vacuum for 1.0 h. Field-effect characteristics of the devices were determined in nitrogen using a Keithley 4200 SCS semiconductor parameter analyzer.

Linear mobility was calculated according to the equation below:

$$I_{DS} = (W/L)C_i\mu(V_{GS} - V_{Th})V_{DS} \quad V_{DS} \ll V_{GS} - V_{Th} \quad (1)$$

The mobility of the OFETs in the saturation region was extracted from the following equation:

$$I_{DS} = \frac{W}{2L}\mu C_i (V_{GS} - V_{Th})^2 \quad (2)$$

Where I_{DS} is the drain electrode collected current; L and W are the channel length and width, respectively; μ is the mobility of the device; C_i is the capacitance per unit area of the gate dielectric layer; V_{GS} is the gate voltage, and V_{Th} is the threshold voltage. The V_{Th} of the device was determined by extrapolating the $(I_{DS,sat})^{1/2}$ vs. V_{GS} plot to $I_{DS} = 0$.

The contact resistance was determined in the following way (a. Luan, S.; Neudeck, G. W. *J. Appl. Phys.* **1992**, 72, 766; b. Lefenfeld, M.; Blanchet, G.; Rogers, J. A. *Adv. Mater.* **2003**, 15, 1188.). For a BGBC FET, the ON resistance, R_{ON} , in the linear operation regime (source-drain voltage \ll gate voltage), can be expressed as follows:

$$R_{on} = \frac{\partial V_{DS}}{\partial I_{DS}} \int_{V_{DS} \rightarrow 0}^{V_{GS}} = R_{ch} + R_p = \frac{L}{W\mu_i C_i (V_{GS} - V_{Th})} + R_p \quad (3)$$

where R_{ch} is the channel resistance, R_p is the parasitic resistance, and V_{GS} is the gate voltage. The parasitic resistance, R_p , which is associated with the contacts between S - D electrode and semiconductor layer, can be extracted by measuring the ON resistance, R_{ON} , from the linear region of the FET output characteristics. We got a plot of R_{ON} as a function of L at the gate voltage of -30 V, and found that the relationship of R_{ON} vs L gives straight lines, indicating that the ON resistance is well expressed by Eq. (3). By extrapolating the relationship of R_{ON} vs L to $L = 0$, the contact resistance values can be determined. The

contact resistances for BGBC devices with thin films of **pDPP4T-1**, **pDPP4T-2**, **pDPP4T-3**, **pDPP4T**, **pDPP4T-A**, **pDPP4T-B** and **pDPP4T-C** were determined to be 0.82 M Ω , 0.21 M Ω , 0.11 M Ω , 1.40 M Ω , 0.71 M Ω , 0.53 M Ω and 0.52 M Ω , respectively.

6. Transfer and Output Curves of BGBC and BGTC Devices with Thin Films of pDPP4T-1, pDPP4T-2, pDPP4T-3, pDPP4T, pDPP4T-A, pDPP4T-B and pDPP4T-C

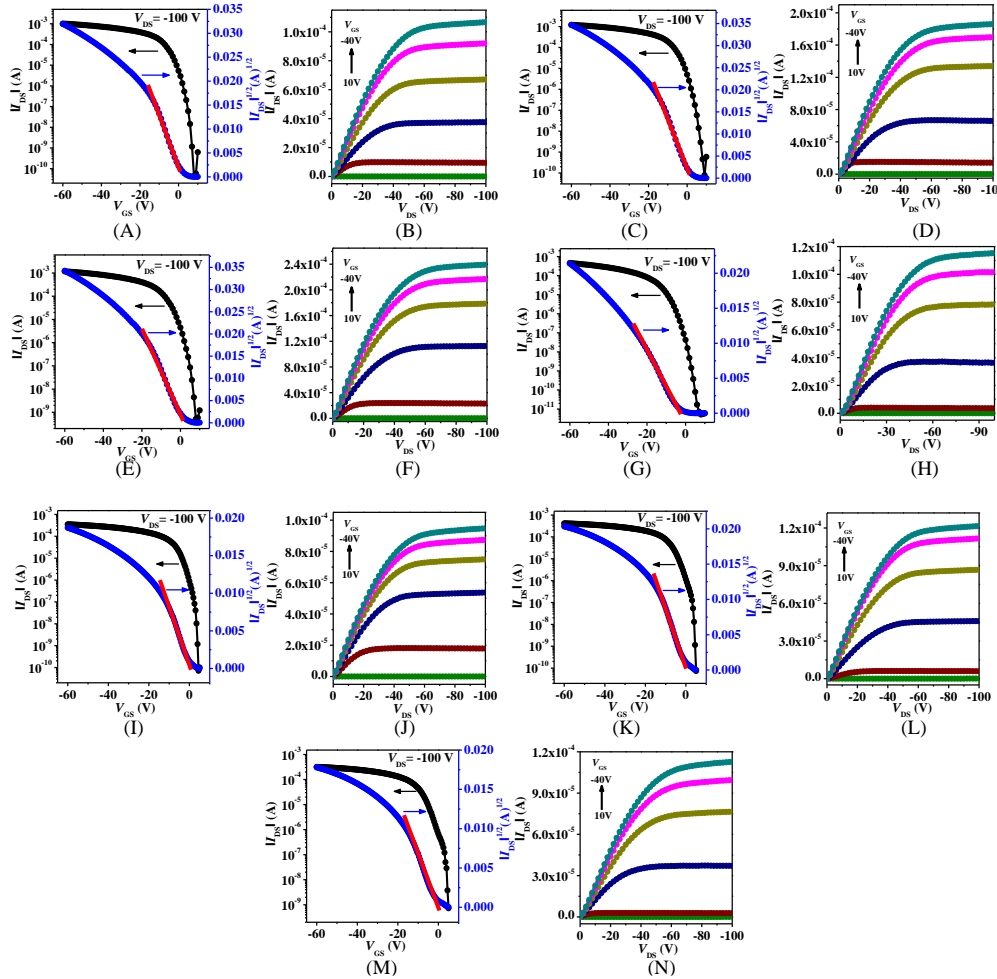


Figure S4. The transfer and output curves of BGBC FETs with thin films of **pDPP4T-1** (A, B), **pDPP4T-2** (C, D), **pDPP4T-3** (E, F), **pDPP4T** (G, H), **pDPP4T-A** (I, J), **pDPP4T-B** (K, L) and **pDPP4T-C** (M, N) after thermal annealing at 100 °C; the channel width (W) and length (L) were 1440 μm and 50 μm , respectively.

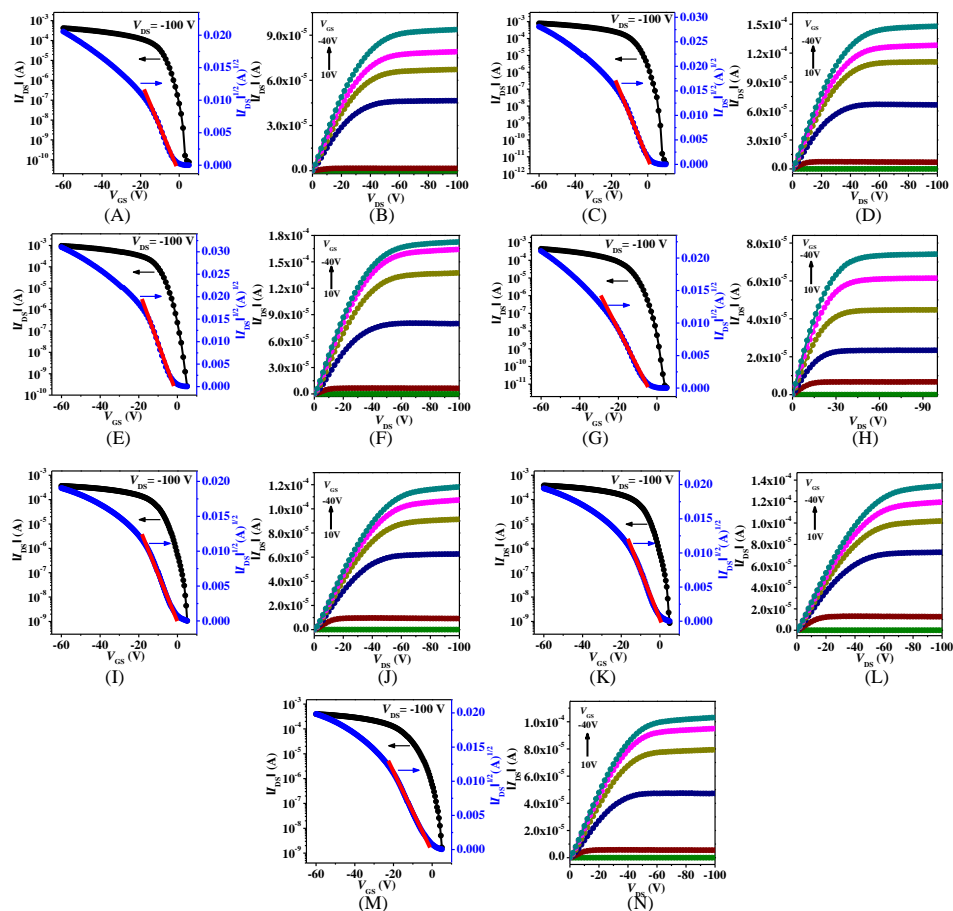


Figure S5. The transfer and output curves of BGTC FETs with thin films of **pDPP4T-1** (A, B), **pDPP4T-2** (C, D), **pDPP4T-3** (E, F), **pDPP4T** (G, H), **pDPP4T-A** (I, J), **pDPP4T-B** (K, L) and **pDPP4T-C** (M, N) after thermal annealing at 100 °C; the channel width (W) and length (L) were 3000 μm and 100 μm , respectively.

Table S2. Hole Mobilities (μ_h), Threshold Voltages (V_{Th}) and $I_{\text{on}}/I_{\text{off}}$ Ratios for BGTC FETs with thin films of **pDPP4T-1**, **pDPP4T-2**, **pDPP4T-3**, **pDPP4T**, **pDPP4T-A**, **pDPP4T-B** and **pDPP4T-C** after Annealing at 100 °C.

polymer	$\mu_h^a / \text{cm}^2 \text{V}^{-1} \text{s}^{-1}$	$V_{\text{Th, h}}/\text{V}$	$I_{\text{on}}/I_{\text{off}}$
pDPP4T-1	4.8/4.4	-3 - 10	$10^6 - 10^7$
pDPP4T-2	6.4/5.9	0 - 9	$10^7 - 10^8$
pDPP4T-3	8.8/7.1	-5 - 10	$10^6 - 10^7$
pDPP4T-A	3.7/3.1	-5 - 8	$10^5 - 10^6$
pDPP4T-B	4.1/3.5	-4 - 9	$10^5 - 10^6$
pDPP4T-C	2.6/2.1	-3 - 10	$10^5 - 10^6$
pDPP4T	2.6/2.2	-5 - 11	$10^7 - 10^8$

^a The mobilities were provided in “highest/average” form, and the performance data were obtained based on more than 10 different FETs.

7. Devices Stability Data

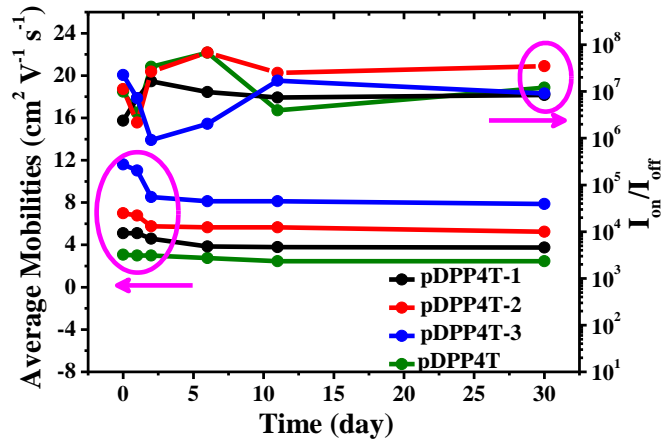


Figure S6. Variation of hole mobilities and I_{on}/I_{off} ratios for BGBC FETs of **pDPP4T-1**, **pDPP4T-2**, **pDPP4T-3** and **pDPP4T** after being left in air for 30 days.

8. 1-D GIXRD Patterns

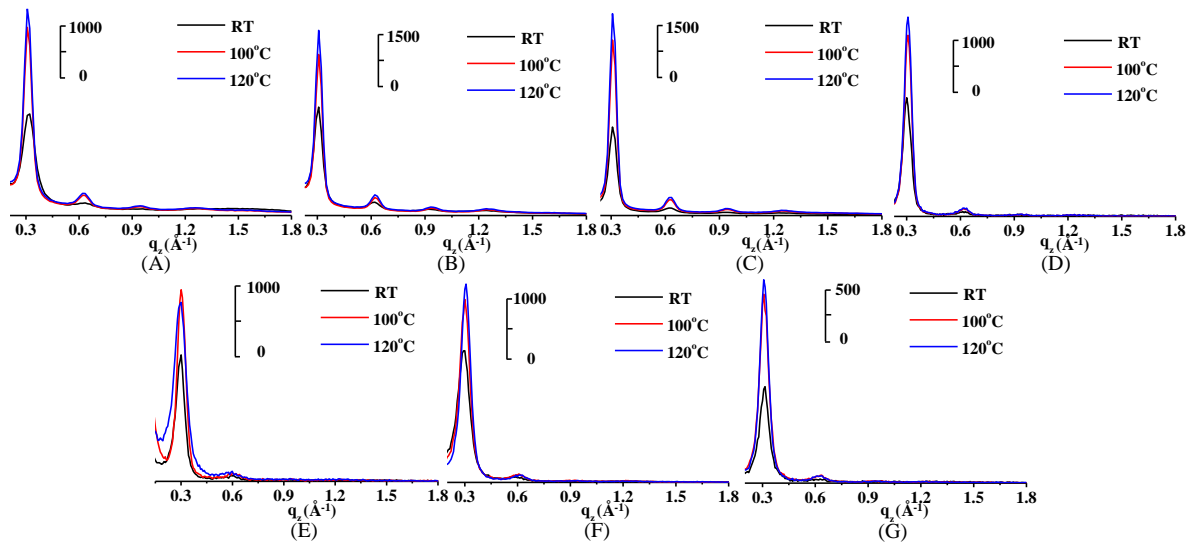


Figure S7. 1-D GIXRD patterns in the *out-of-plane* direction for **pDPP4T-1** (A), **pDPP4T-2** (B), **pDPP4T-3** (C), **pDPP4T** (D) and **pDPP4T-A** (E), **pDPP4T-B** (F) and **pDPP4T-C** (G) deposited on OTS-modified SiO_2/Si substrates after thermal annealing at different temperatures.

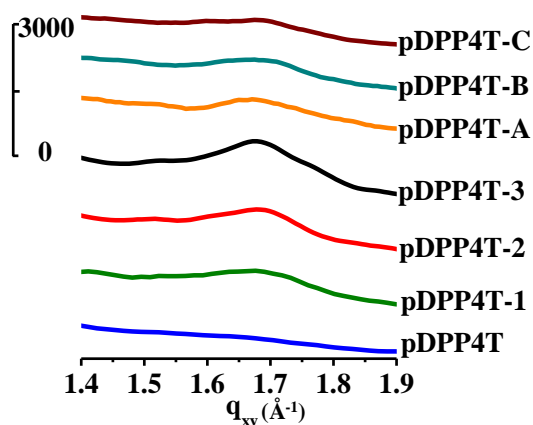


Figure S8. 1-D GIXRD patterns in the *in-plane* direction for **pDPP4T-1**, **pDPP4T-2**, **pDPP4T-3**, **pDPP4T**, **pDPP4T-A**, **pDPP4T-B**, and **pDPP4T-C** deposited on OTS-modified SiO₂/Si substrates after thermal annealing at 100 °C.

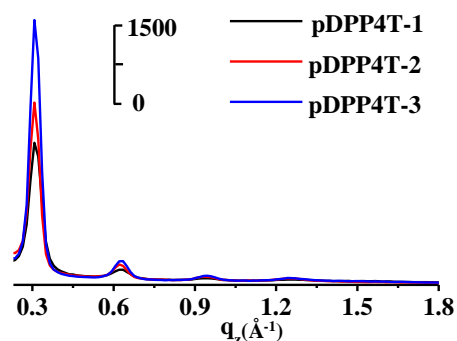


Figure S9. 1-D *out-of-plane* X-ray diffraction patterns of **pDPP4T-1**, **pDPP4T-2** and **pDPP4T-3** after thermal annealing at 100 °C.

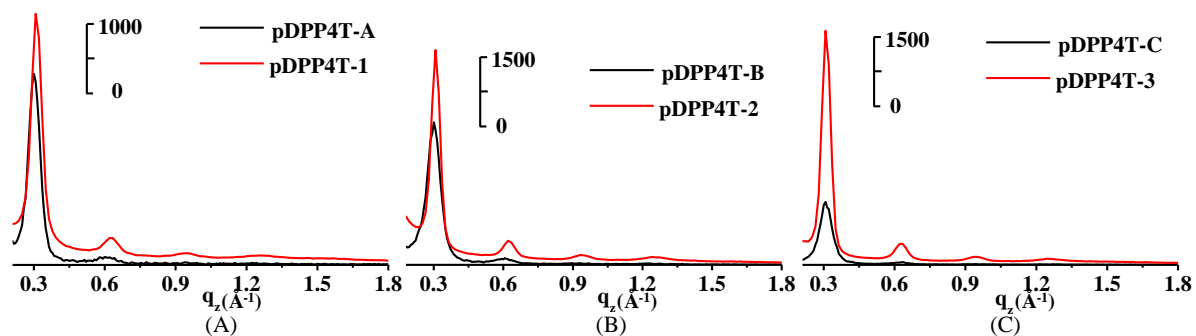


Figure S10. 1-D *out-of-plane* X-ray diffraction patterns of **pDPP4T-1** and **pDPP4T-A** (A), **pDPP4T-2** and **pDPP4T-B** (B) and **pDPP4T-3** and **pDPP4T-C** (C) after thermal annealing at 100 °C.

9. AFM Images of pDPP4T-A, pDPP4T-B and pDPP4T-C

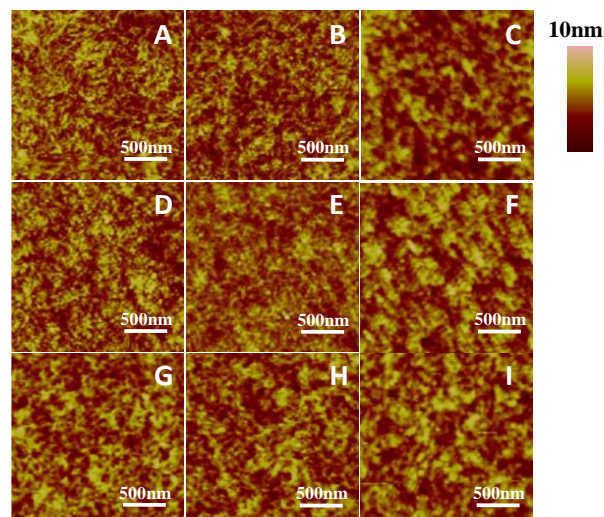


Figure S11. AFM height images of thin films of **pDPP4T-A** (A, D, G), **pDPP4T-B** (B, E, H) and **pDPP4T-C** (C, F, I) deposited on OTS-modified SiO₂/Si substrates at room temperature (*up*) and after thermal annealing at 100 °C (*middle*) and 120 °C (*down*).

10. Fabrication of Organic Photovoltaic Cells

OPVs were fabricated with ITO as the positive electrode and Al as the negative electrode. The patterned indium tin oxide (ITO) glass (sheet resistance = 15 Ω/square) was pre-cleaned in an ultrasonic bath in detergent, deionized water, acetone and isopropyl alcohol, then treated in an ultraviolet-ozone chamber (Jelight Company, USA) for 30 min. A thin layer (30 nm) of poly(3,4-ethylenedioxythiophene):poly(styrenesulfonate) (PEDOT:PSS, Baytron PVP AI 4083, Germany) was spin-coated onto the ITO glass and baked at 150 °C for 15 min. Blend solutions were prepared in different solvents at a total concentration of 15-18 mg/ml (donor/acceptor weight ratio: 1/2 or 1/1) and stirred 2 hours for complete dissolution. Then, the **pDPP4T**, **pDPP4T-1**, **pDPP4T-2**, **pDPP4T-3**, **pDPP4T-A**, **pDPP4T-B** and **pDPP4T-C/PC₇₁BM** blend solution was spin-coated. The thickness (ca.

100-120 nm) of the active layer was measured using an Ambios Technology XP-2 profilometer. Ca (ca. 20 nm) and aluminum layer (ca. 70 nm) were then evaporated onto the surface of the active layer under vacuum (ca. 10^{-5} Pa) to form the negative electrode respectively. The active area of the device was 5.0 mm^2 . The J - V curves were measured with a computer-controlled Keithley 236 Source Measure Unit. A xenon lamp coupled with AM 1.5 solar spectrum filters was used as the light source, and the optical power at the sample was 100 mW cm^{-2} . The incident photon to converted current efficiency (IPCE) spectra were performed at Solar Cell Spectral Response Measurement System QE-R3011 (EnliTechnololy Co. Ltd).

11. J - V Curves and IPCE Spectra of pDPP4T-A, pDPP4T-B and pDPP4T-C with PC₇₁BM

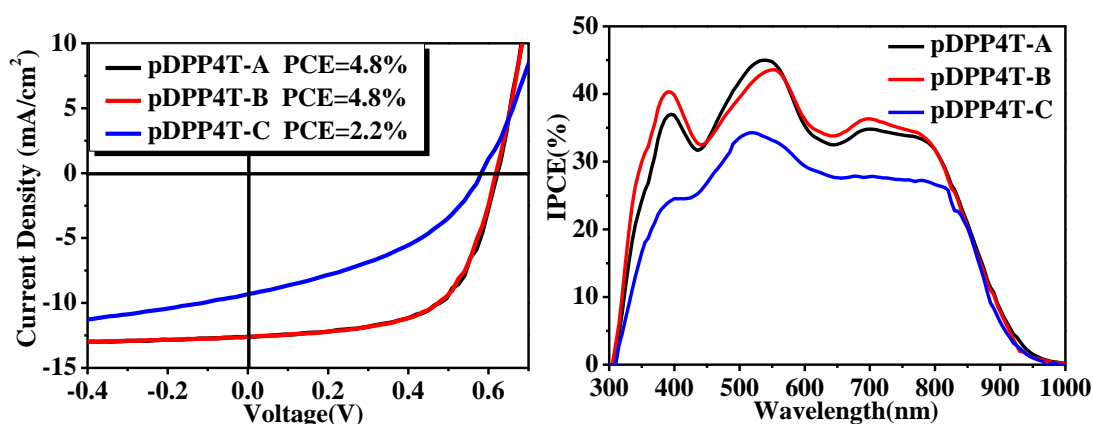
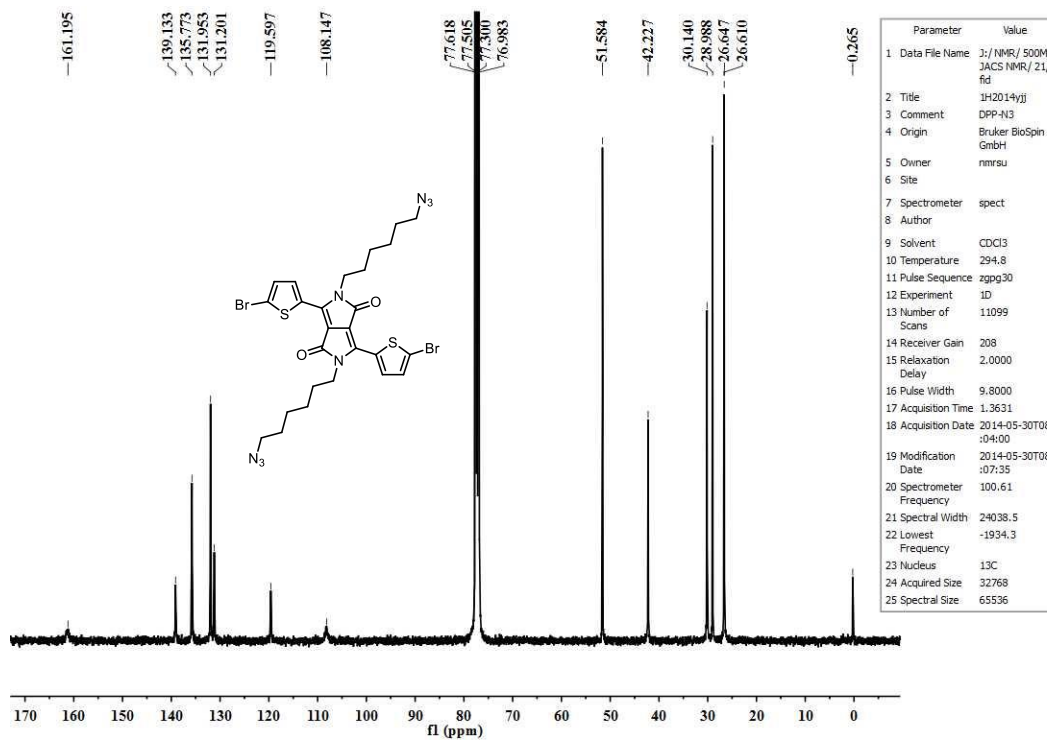
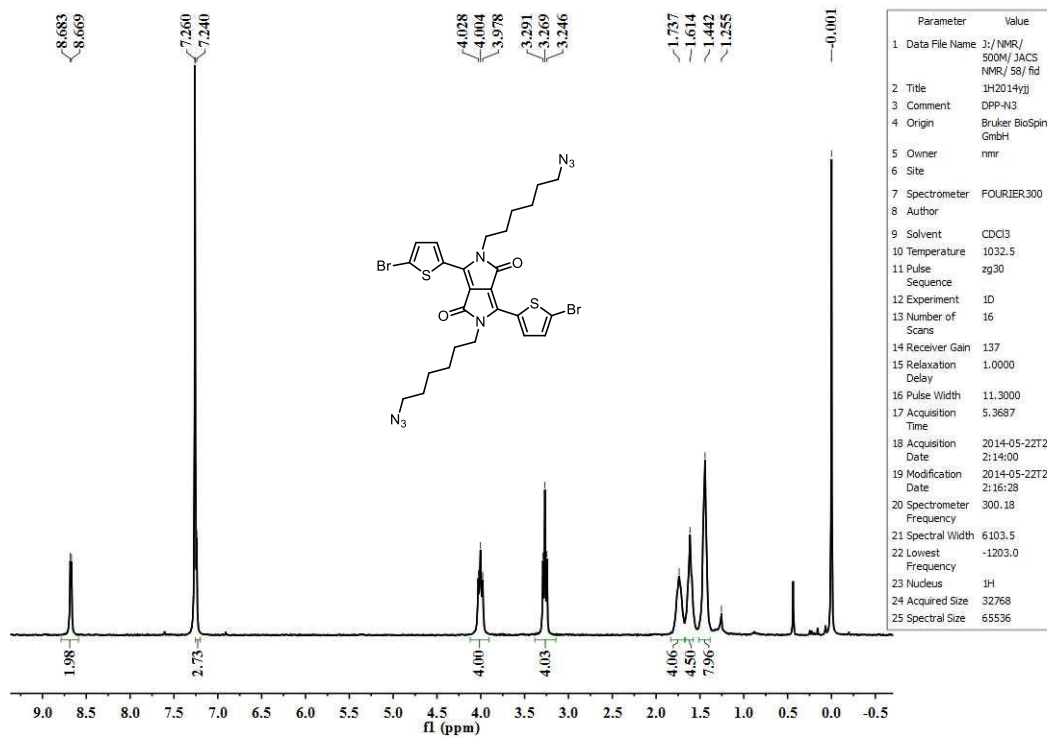


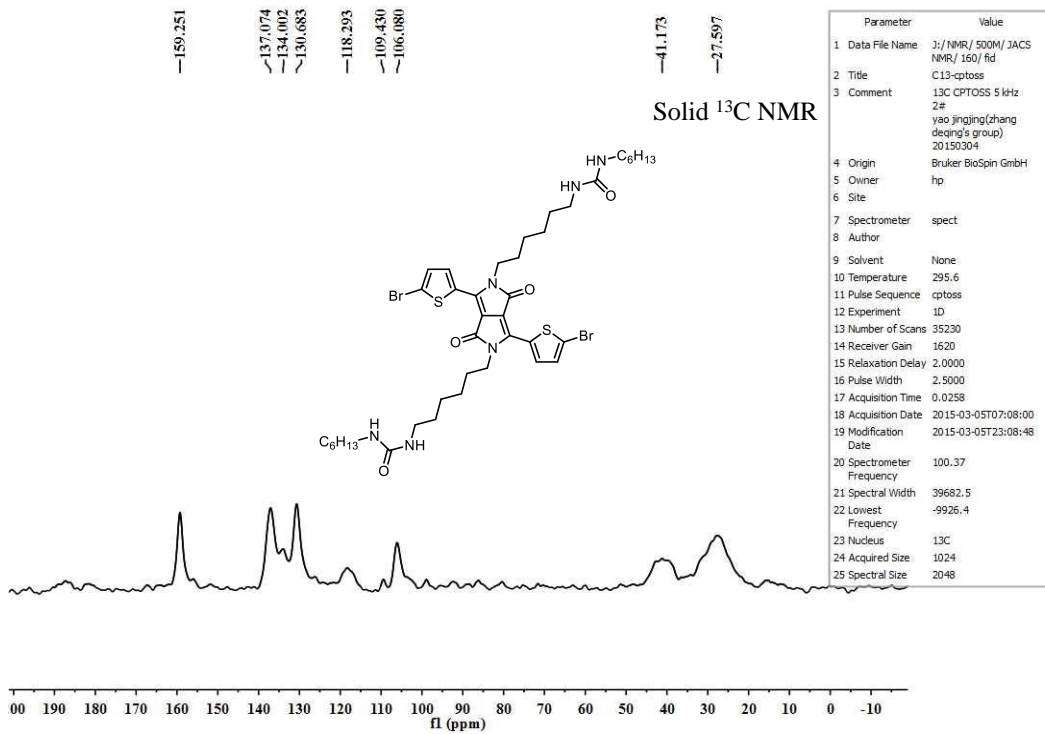
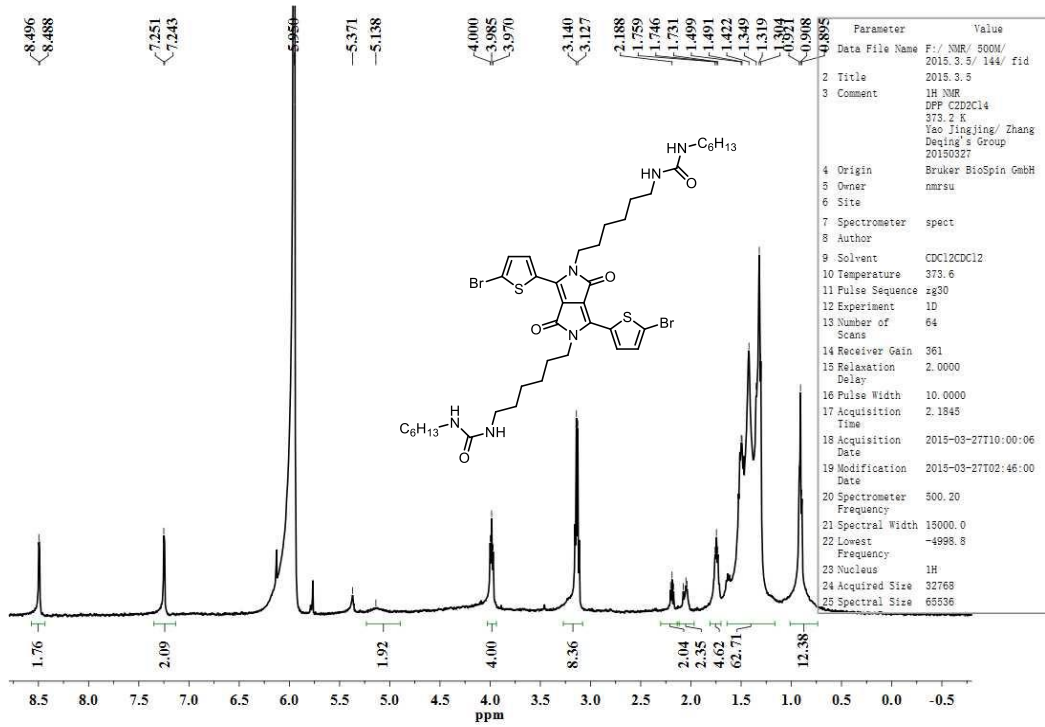
Figure S12. J - V curves (*left*) and IPCE spectra (*right*) of photovoltaic cells with the respective blend films of pDPP4T-A, pDPP4T-B and pDPP4T-C with PC₇₁BM at 1:2 weight ratio under AM 1.5 illumination (100 mW/cm^2).

12. ¹HNMR and ¹³CNMR Spectra

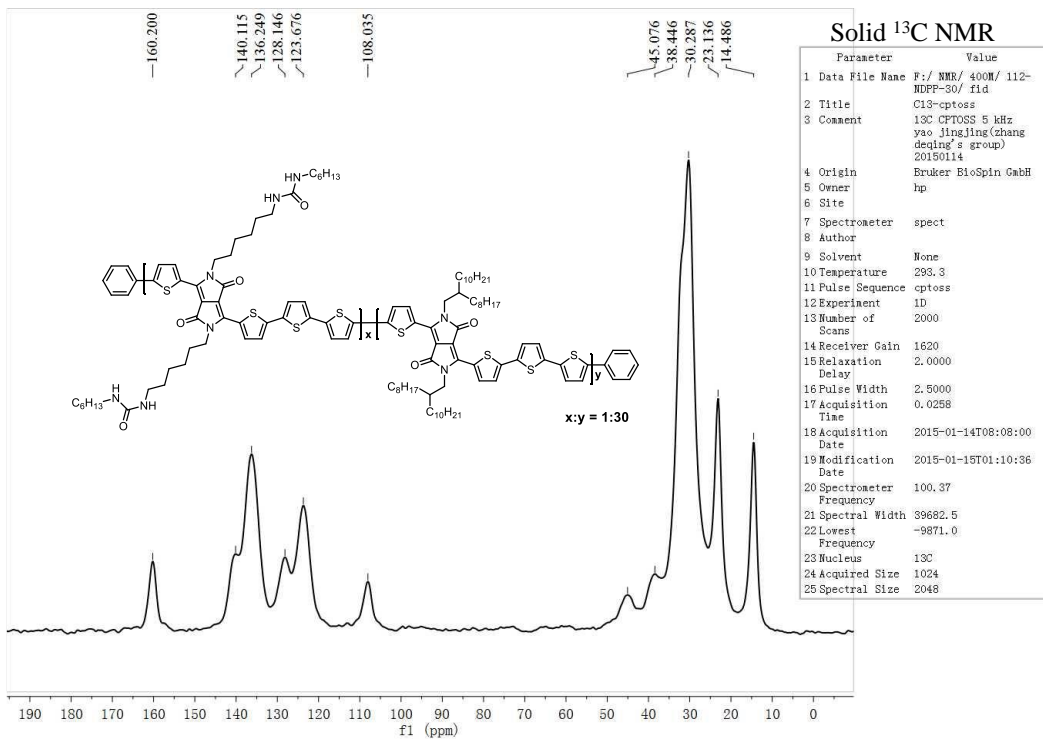
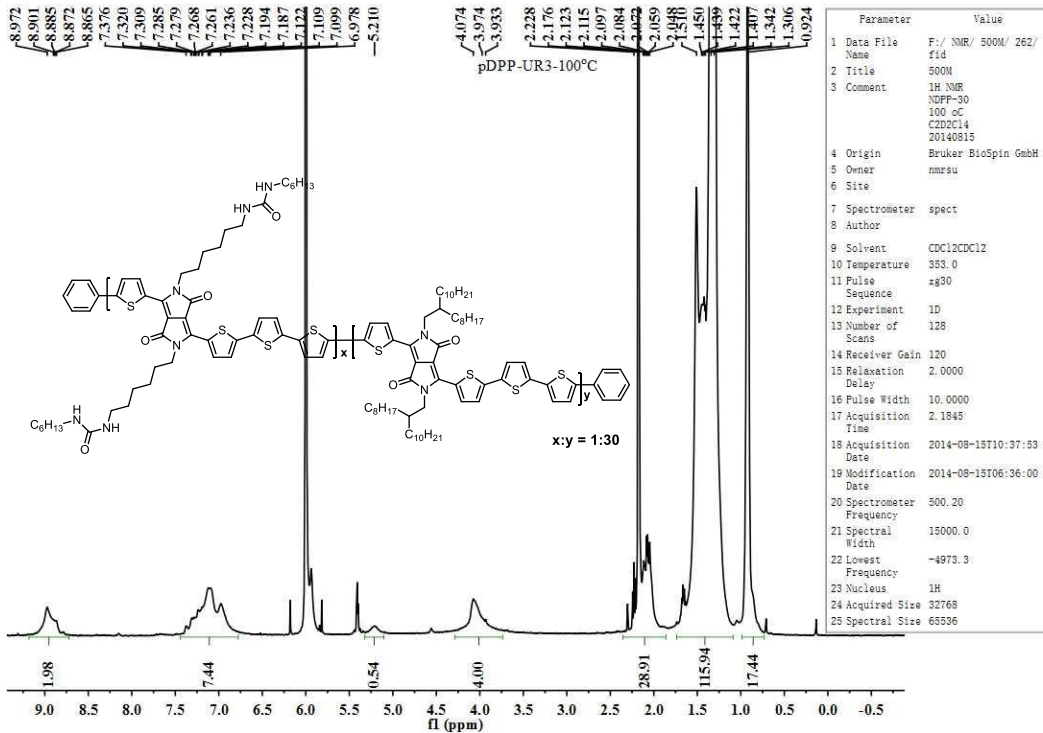
Compound 5



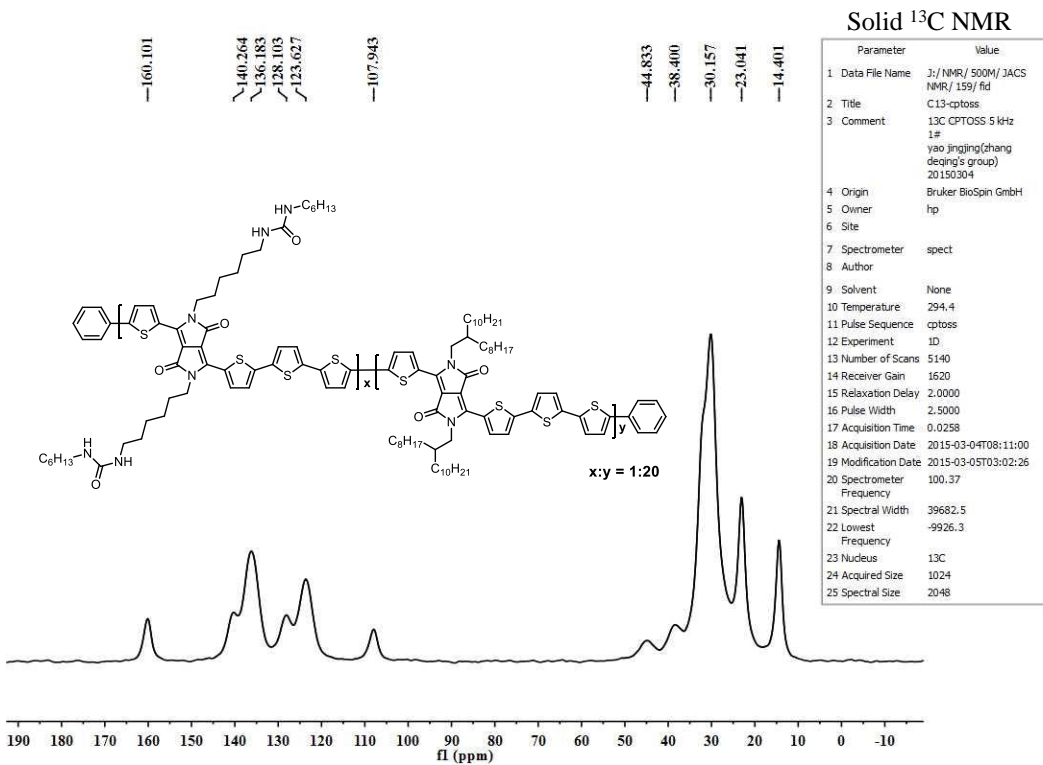
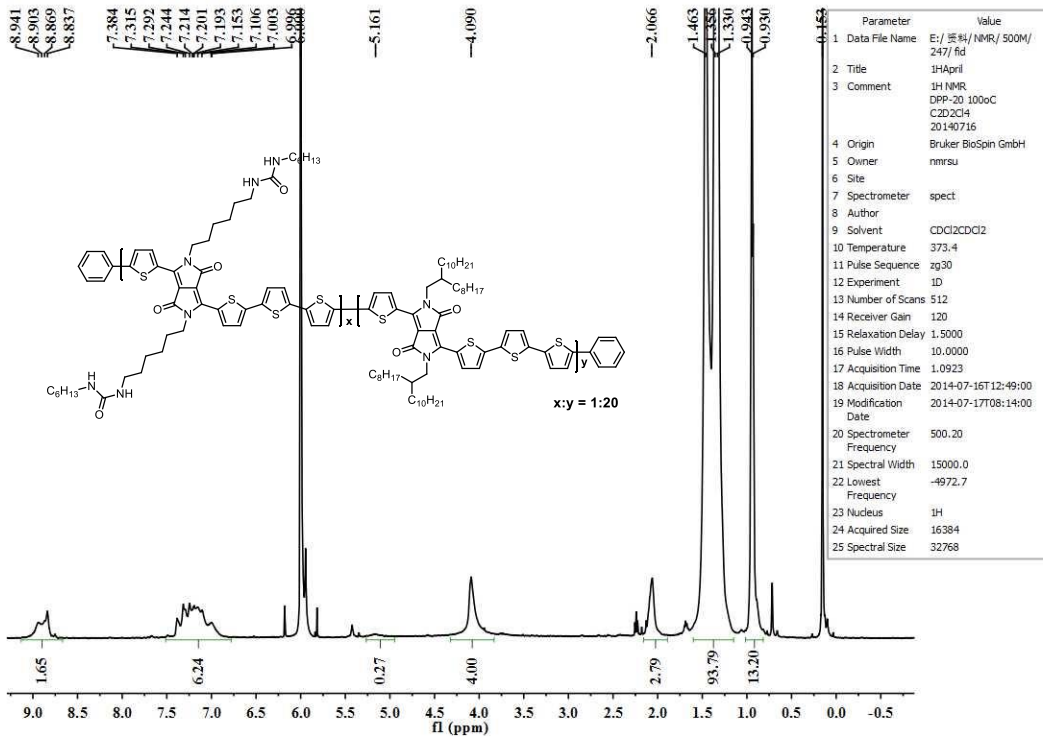
Compound 1



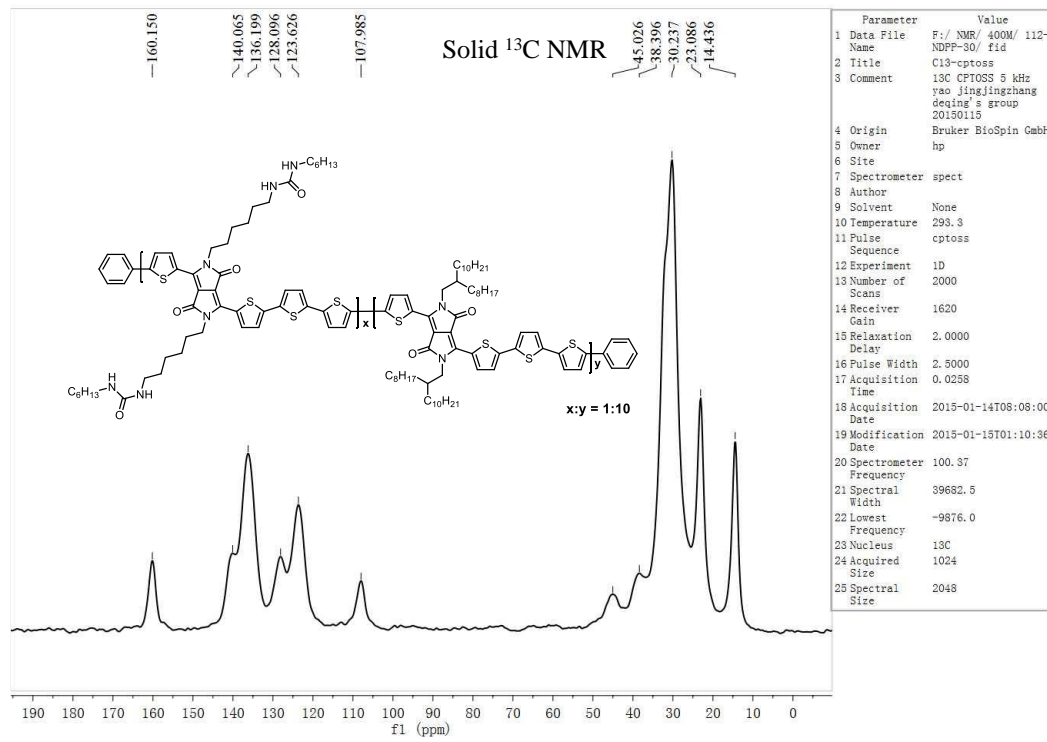
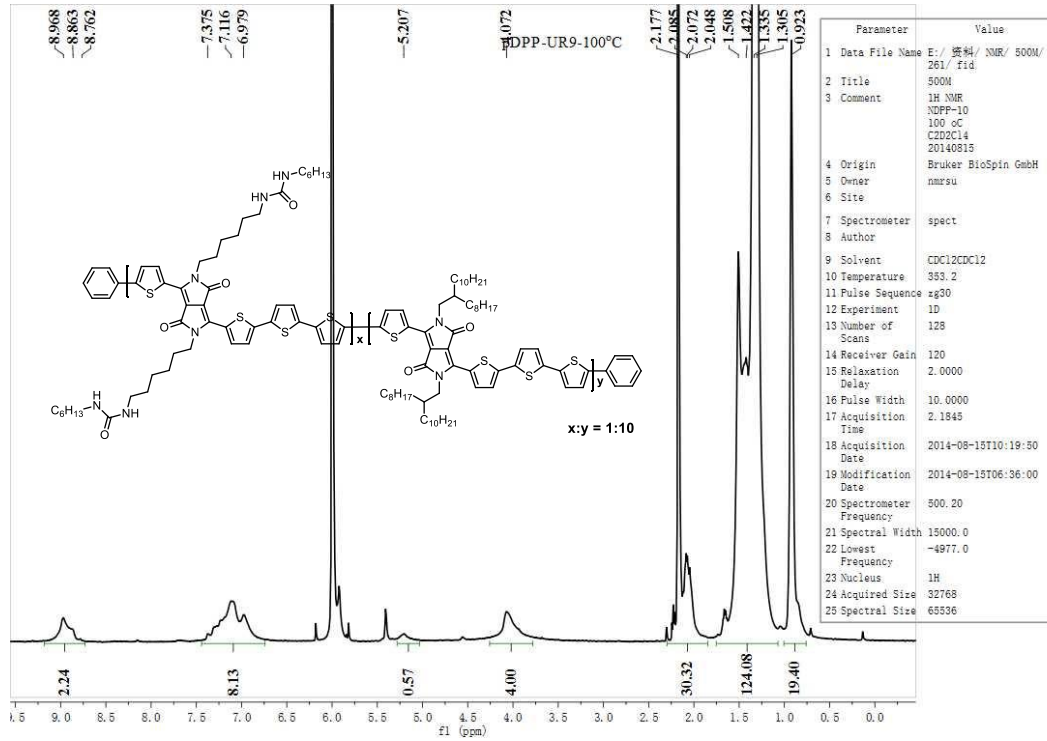
pDPP4T-1



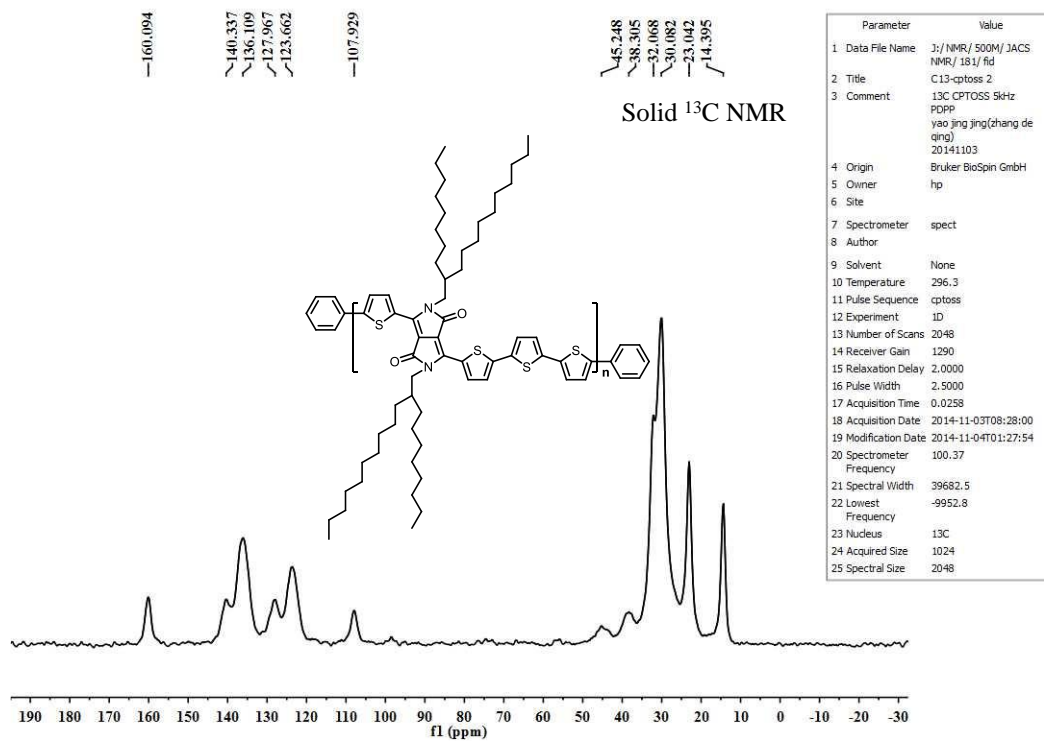
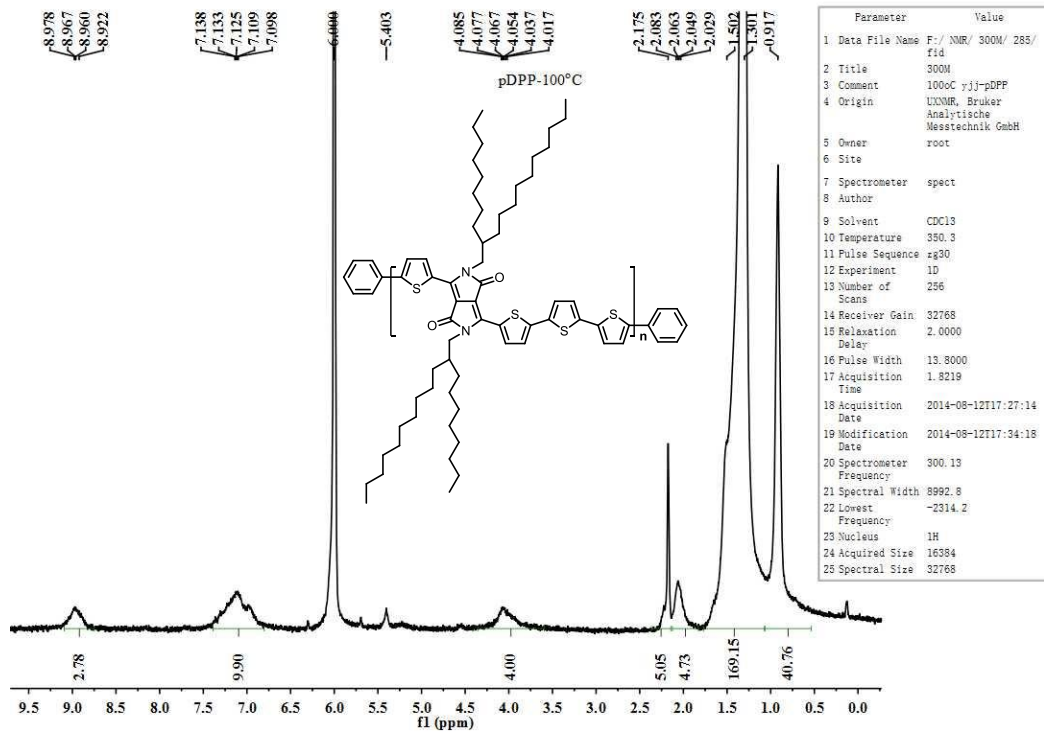
pDPP4T-2



pDPP4T-3

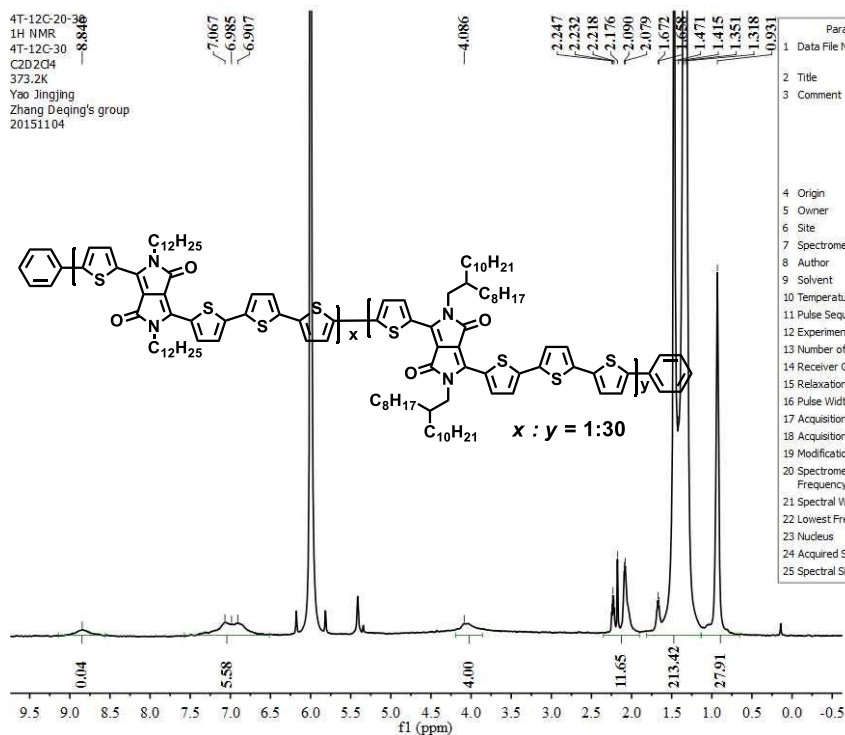


pDPP4T



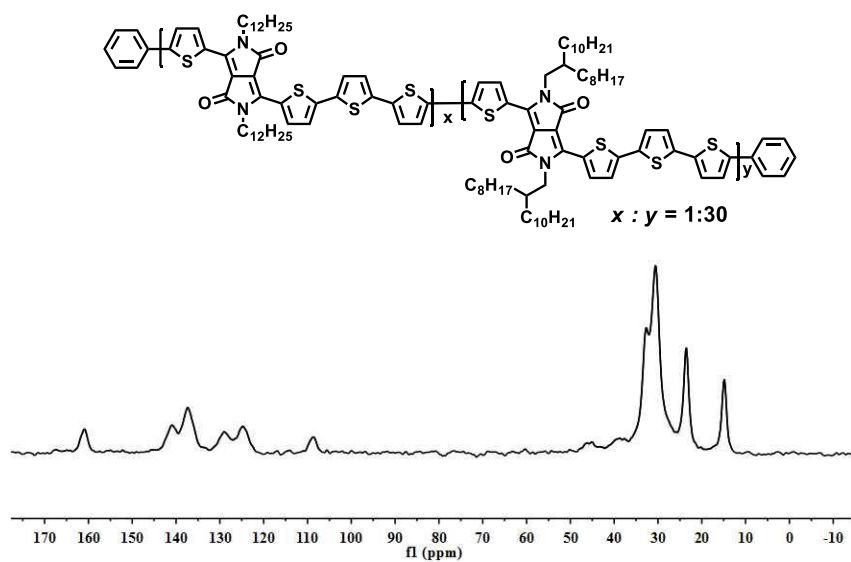
pDPP4T-A

4T-12C-20-30
 1H NMR
 4T-12C-30
 C2D2Cl4
 373.2K
 Yao Jingjing
 Zhang Deqing's group
 20151104



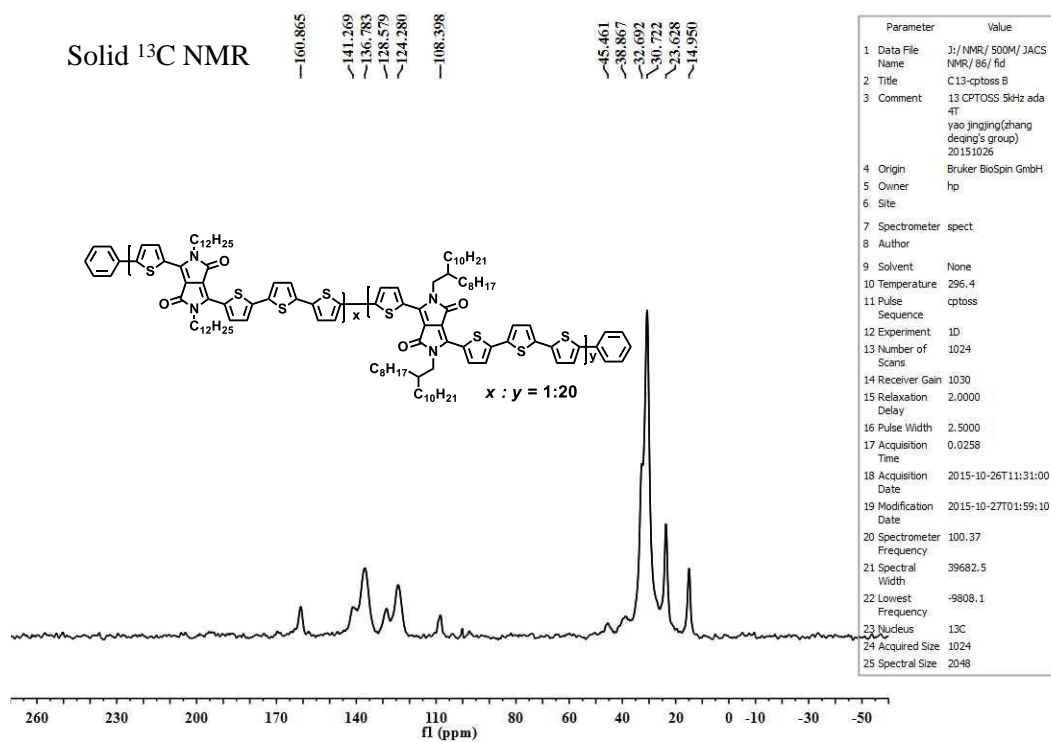
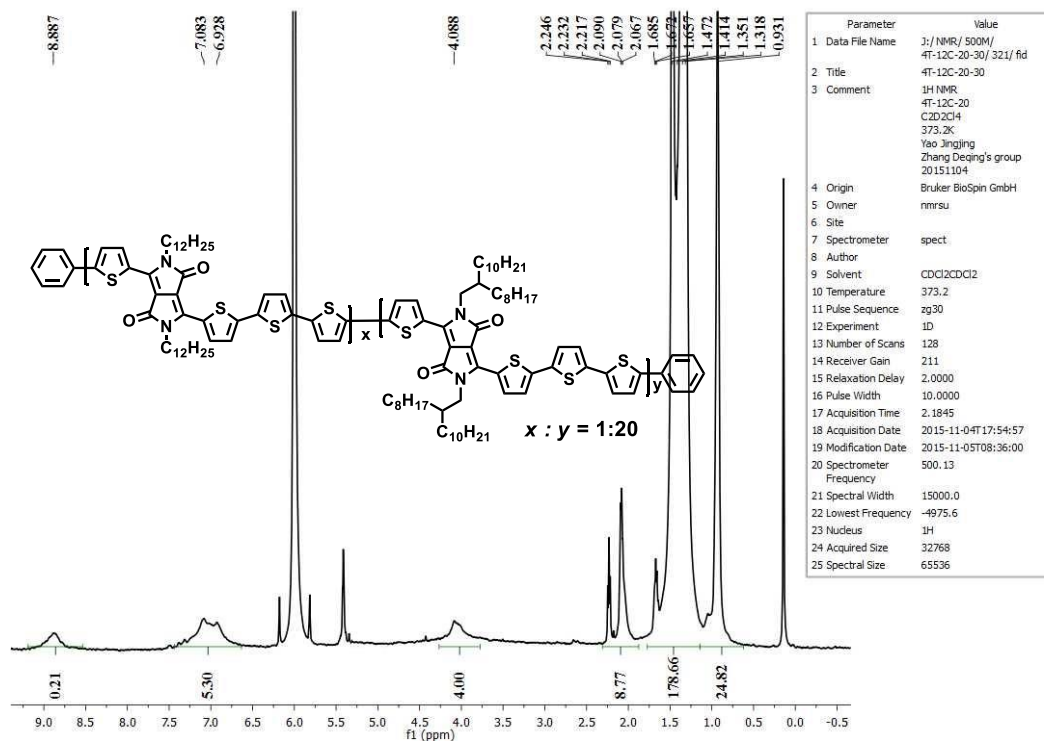
Parameter	Value
1 Data File Name	J:/NMR/500M/4T-12C-20-30/322/ fid
2 Title	4T-12C-20-30
3 Comment	1H NMR 4T-12C-30 C2D2Cl4 373.2K Yao Jingjing Zhang Deqing's group 20151104
4 Origin	Bruker BioSpin GmbH
5 Owner	nmrsu
6 Site	
7 Spectrometer	spect
8 Author	
9 Solvent	CDCl2CDC12
10 Temperature	373.3
11 Pulse Sequence	zg30
12 Experiment	1D
13 Number of Scans	128
14 Receiver Gain	211
15 Relaxation Delay	2.0000
16 Pulse Width	10.0000
17 Acquisition Time	2.1845
18 Acquisition Date	2015-11-04T22:23:11
19 Modification Date	2015-11-05T08:36:00
20 Spectrometer Frequency	500.13
21 Spectral Width	15000.0
22 Lowest Frequency	-4975.6
23 Nucleus	1H
24 Acquired Size	32768
25 Spectral Size	65536

160.911
 140.908
 137.332
 129.011
 124.778
 108.669
Solid ¹³C NMR
 45.097
 38.651
 37.665
 32.655
 30.570
 23.551
 14.871

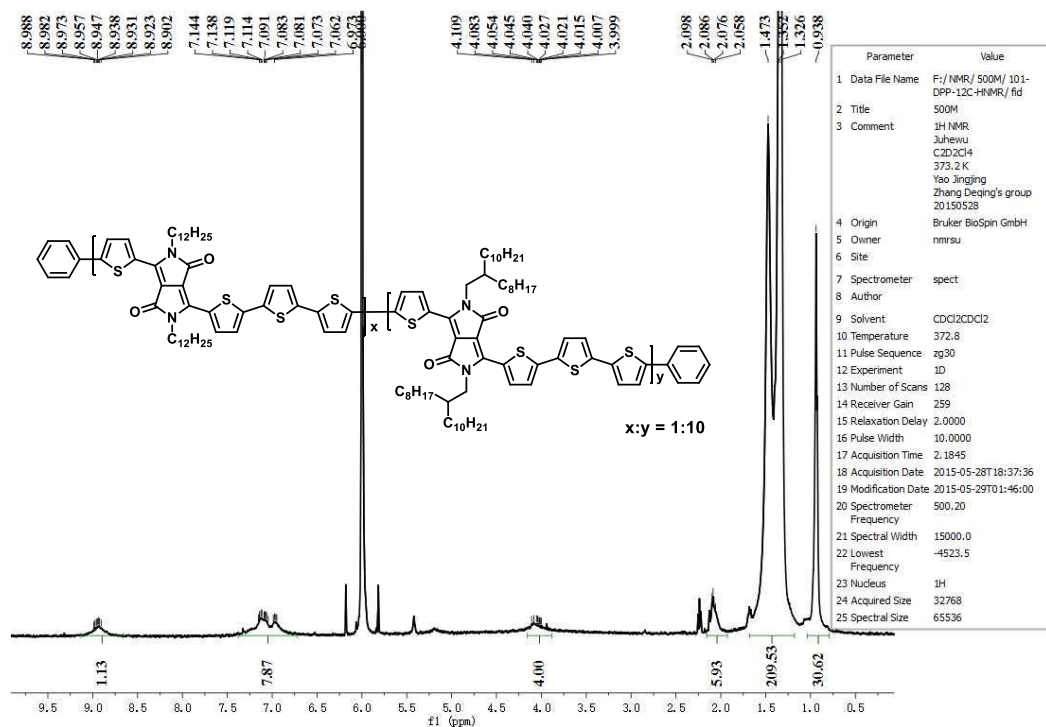


Parameter	Value
1 Data File Name	J:/NMR/500M/JACS Name/85/ fid
2 Title	C13-cptoss B
3 Comment	13 CPTOSS 5kHz ada 3T yao jingjing(zhang deqing's group) 20151026
4 Origin	Bruker BioSpin GmbH
5 Owner	hp
6 Site	
7 Spectrometer	spect
8 Author	
9 Solvent	None
10 Temperature	296.5
11 Pulse Sequence	cptoss
12 Experiment	1D
13 Number of Scans	1024
14 Receiver Gain	1030
15 Relaxation Delay	2.0000
16 Pulse Width	2.5000
17 Acquisition Time	0.0258
18 Acquisition Date	2015-10-26T10:52:00
19 Modification Date	2015-10-27T01:13:20
20 Spectrometer Frequency	100.37
21 Spectral Width	39682.5
22 Lowest Frequency	-9809.9
23 Nucleus	13C
24 Acquired Size	1024
25 Spectral Size	2048

pDPP4T-B



pDPP4T-C



Solid ¹³C NMR

